SIMS CHEMICAL ANALYSIS OF EXTENDED IMPACTS ON THE LEADING AND TRAILING EDGES OF LDEF EXPERIMENT AO187-2

S. Amari, J. Foote, P. Swan, R. M. Walker, E. Zinner
McDonnell Center for the Space Sciences and Physics Department
Washington University
One Brookings Drive
St. Louis, MO 63130-4899
Phone: 314/935-6257, Fax: 314/935-6219

G. Lange
Max-Planck-Institut für Kernphysik
Postfach 103980
D-6900 Heidelberg, Germany
Phone: 6221 516 247, Fax: 6221 516 540

SUMMARY

Numerous "extended impacts" found in both leading and trailing edge capture cells have been successfully analyzed for the chemical composition of projectile residues by secondary ion mass spectrometry (SIMS). Most data have been obtained from the trailing edge cells where 45 of 58 impacts have been classified as "probably natural" and the remainder as "possibly man-made debris." This is in striking contrast to leading edge cells where 9 of 11 impacts so far measured are definitely classified as orbital debris. Although all the leading edge cells had lost their plastic entrance foils during flight, the rate of foil failure was similar to that of the trailing edge cells, 10% of which were recovered intact. Ultra-violet embrittlement is suspected as the major cause of failure on both leading and trailing edges. The major impediment to the accurate determination of projectile chemistry is the fractionation of volatile and refractory elements in the hypervelocity impact and redeposition processes. This effect had been noticed in a simulation experiment but is more pronounced in the LDEF capture cells, probably due to the higher average velocities of the space impacts. Surface contamination of the pure Ge surfaces with a substance rich in Si but also containing Mg and Al provides an additional problem for the accurate determination of impactor chemistry. The effect is variable, being much larger on surfaces that were exposed to space than in those cells that remained intact. Future work will concentrate on the analyses of more leading edge impacts and the development of new SIMS techniques for the measurement of elemental abundances in extended impacts.

INTRODUCTION

LDEF experiment A0187-2 consisted of 228 Ge-mylar cells for the capture of interplanetary dust material. The principle of the experiment and a more detailed description of the capture cells is given by Amari et al. (ref. 1). One full tray of capture cells was exposed on the leading edge and an area equivalent to a full tray in two locations on the trailing edge.

All cells on the leading edge and 90% of the cells on the trailing edge had lost their plastic covers (bare cells) during exposure in space. However, Ge plates from both leading and trailing edge bare cells contain extended impact features that must have been produced by high velocity projectiles while the mylar foils were still intact. Moreover, these extended impact features contain projectile material that could be measured by secondary ion mass spectrometry (SIMS), an extremely sensitive surface analysis technique.

Last year we reported results of the optical scanning of 100 bare cells from the trailing edge as well as the first results of SIMS analysis of 24 extended impacts on Ge from these cells (ref. 1). In the present paper we extend the SIMS analysis to 16 additional impacts from bare trailing edge cells and 18 impacts from the 12 trailing edge cells that had retained their plastic covers. We also optically scanned the Ge plates of 106 capture cells from the leading edge for single craters and extended impacts and analyzed 11 of the latter by SIMS.

OPTICAL SCANNING FOR SINGLE CRATERS AND EXTENDED IMPACTS

All cells were optically scanned under oblique illumination at a magnification of 240× as previously described by Amari *et al.* (ref. 1). The results are given in Table 1. There is a clear distinction between "extended impact features" and "single craters." The former consist of complex patterns of debris and ejecta, and must have been produced while the plastic cover foils were in place. In contrast, "single craters" show no evidence of associated debris deposits and represent direct hits on the Ge plates after the foils had failed in flight. The distinction between "extended impacts A and B" is subjective with the former generally being larger than the latter and being visible with the unaided eye. Although we have chosen to analyze the type A impacts first, we consider it likely that also many of the type B impacts contain sufficient material for chemical and isotopic analysis.

Table 1. Analysis of Cells on AO187-2

	Cells scanned	Single Craters	Extended Impacts A	Extended Impacts B	Measured by SIMS	
					Ge	Foil
Trailing Edge Bare	100	203	53	155	40	
Trailing Edge Covered	12	-	20	26	18	5
Leading Edge	106	5121	403	298	11	

There are several differences between the impacts on the two sides of the spacecraft. Figure 1 shows histograms of the sizes of extended impacts on the leading and trailing edge cells. As can be seen, the trailing edge impacts have, on average, much larger diameters than those on the leading edge. This is undoubtedly a reflection of the lower projectile velocities and shallower impact directions (ref. 2) for the trailing edge. An additional reason could be differences in the chemical compositions and physical properties of the projectiles, since a large fraction of leading edge impacts appear to be caused by man-made debris (see below), while those on the trailing edge are predominately produced by cosmic dust particles.

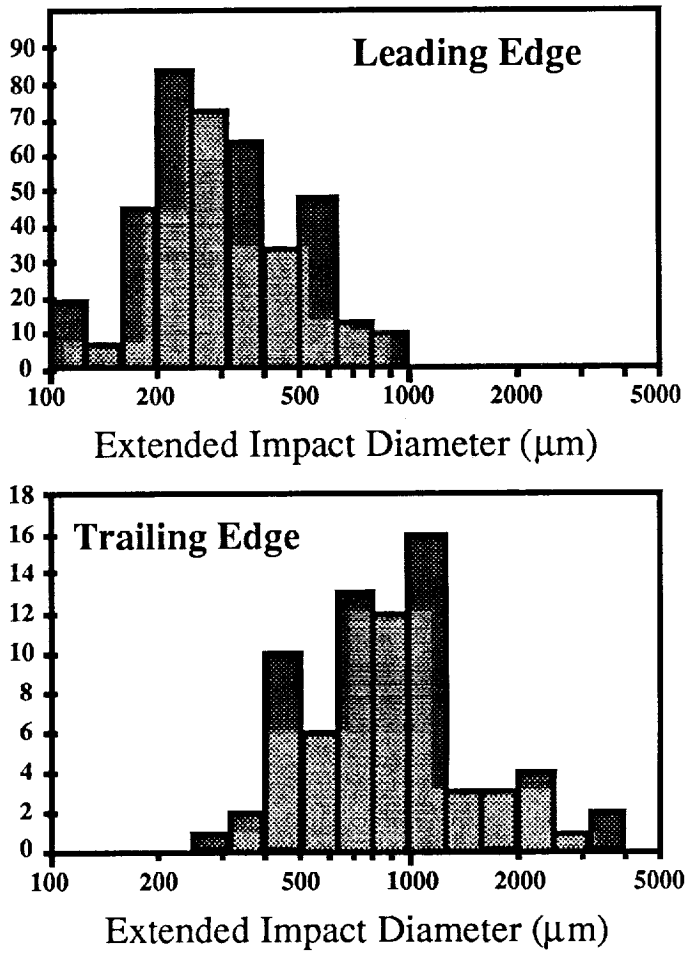

Fig. 1. Distribution of the sizes of extended impacts on Ge plates for both leading and trailing edge capture cells.

LIFETIMES OF ENTRANCE FOILS - FRONT AND BACK

All of the plastic cover foils on the leading edge failed during flight while ~ 10% on those of the trailing edge survived. At first glance it thus appears that there may have been a qualitative difference in the foil destruction processes between front and back. However, as we will show below, this is a somewhat misleading impression. While it is true that the foil loss occurred at a higher rate on the leading edge, foils on this edge lasted for long periods of time in space. The difference in foil survival between front and back is thus more quantitative than qualitative.

Although some corners and edges of many cells contained small pieces of intact or rolled up foil material, when different foils ruptured they appear to have done so suddenly, exposing a major part of the area of any given cell to free space. Since direct hits producing single craters are possible only after the foil has been removed, the density of single craters in a given cell is proportional to the time it was exposed without a foil provided, of course, that the flux of impacting particles is constant in time.

Consider first the results from the leading edge cells. Although none of the plastic foils survived for the entire exposure, it is clear that many remained in place for a considerable period of time. In Fig. 2, we show a histogram of the number of single craters per cell. The width of the distribution far exceeds that expected for a single exposure time for all cells and indicates, in itself, a distribution of survival times. The locations of individual impacts were plotted for the two cells with the largest density of single craters. No clustering was seen, consistent with the assumption that single craters represent a random population of impinging particles.

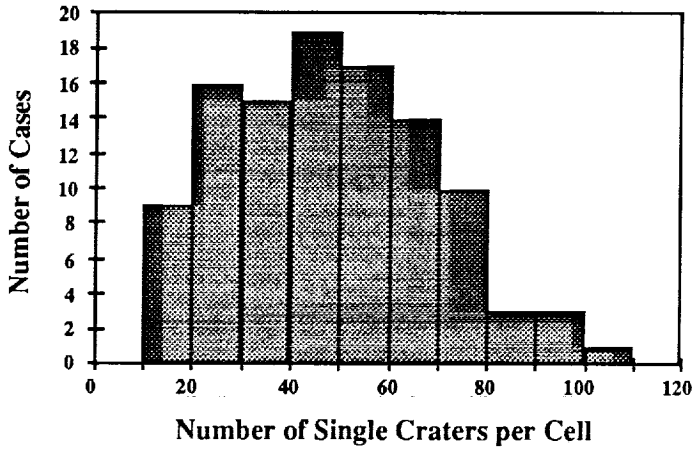

Fig. 2. Distribution of the number of single craters per cell for leading edge capture cells. Such craters are produced only after the entrance foils have ruptered and their numbers are a measure of the time different Ge surfaces were exposed to space. The width of this distribution indicates a considerable spread in foil lifetimes.

The maximum number of single craters per cell is 101. If we assume that the foil on this cell failed immediately after launch, the distribution of craters in Fig. 2 would indicate that more than 50% of the foils survived at least to the half way mark and that some foils lasted through almost 90% of the total exposure time before rupturing.

In contrast to single craters, the density of extended impacts is a measure of the time the foils remained in place. However, only a small fraction of the particles that produce single craters produce extended impacts that are visible under the same scanning conditions. Thus the statistics on extended impacts are less favorable than those for single craters. Figure 3 is a scatter diagram showing the relation between extended impacts (A plus B) and single craters. This figure also shows the same data after binning into groups of 20 single craters and averaging the number of extended impacts in each bin. The data show the expected inverse relationship between number of extended impacts and number of single craters (Fig. 3). Furthermore, the best-fit line through these binned averages intercepts the abscissa at 111 craters per cell, not very different from the maximum number of 101

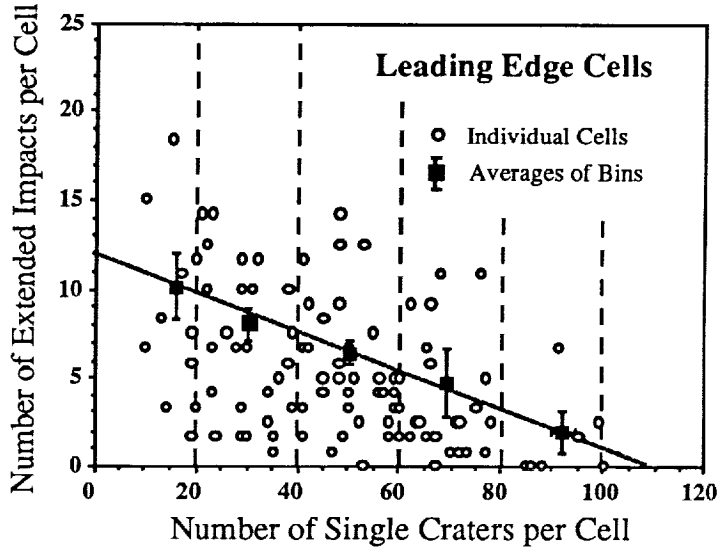

Fig. 3. Extended impacts and single craters for leading edge capture cells. The solid squares show averages for the number of extended impacts versus single crater counts binned in groups of 20. Since extended impacts are produced only when the entrance foils are intact and single impacts only after they have ruptured, there is an inverse correlation between the two densities.

we assumed to be the number of craters on a cell whose foil was removed right after the launch of LDEF. Thus the two indicators of foil lifetimes yield consistent results and a sizable fraction of the foils on the leading edge survived a considerable fraction of the total time of LDEF in orbit.

Consider next the data on the trailing edge cells. The 12 cells which remained covered during the entire period have a total of 46 extended impacts of types A and B for an average of 3.8 impacts/cell. The bare cells have an average of 2.1 extended impacts/cell, suggesting that the foils lasted, on average, about half of the total time. This is similar to the result inferred for the leading edge cells from consideration of the single impact crater data. The first order conclusion is thus that the foil failure rates are similar for both the leading and trailing edge cells.

While we do not know in detail what caused the foils to fail, certain general aspects of the problem seem clear. Firstly, since the rates at which the foils failed were approximately the same for both the leading and trailing edges, the same causative factors must be present. Thus neither atomic oxygen erosion nor enhanced impact fluxes, which are characteristic of the front side only, appears to be the principal cause of failure. However, both effects could have contributed to an enhanced failure rate of the leading edge cells.

Some contribution of atomic oxygen erosion indeed seems likely since we have evidence that most impacts alone do not destroy foils. This conclusion is based on the presence of peculiar elliptical features that accompany approximately half of the extended impacts on the leading edge. Fig. 4 shows two such features that are associated with extended impacts. The fact that these elliptical features occur only on the leading edge Ge plates and only in connection with extended impacts indicates that they must have been caused by the interaction of the residual atmosphere, mostly atomic oxygen, with the penetration hole left by the high velocity impact. At present we do not have any detailed understanding of this process.

Foil failure probably results from repeated stressing of the foils due to cyclical temperature changes, coupled with degradation of the mechanical properties of the foils in the space environment. In spite of the fact that the plastic was metal-coated, we consider UV

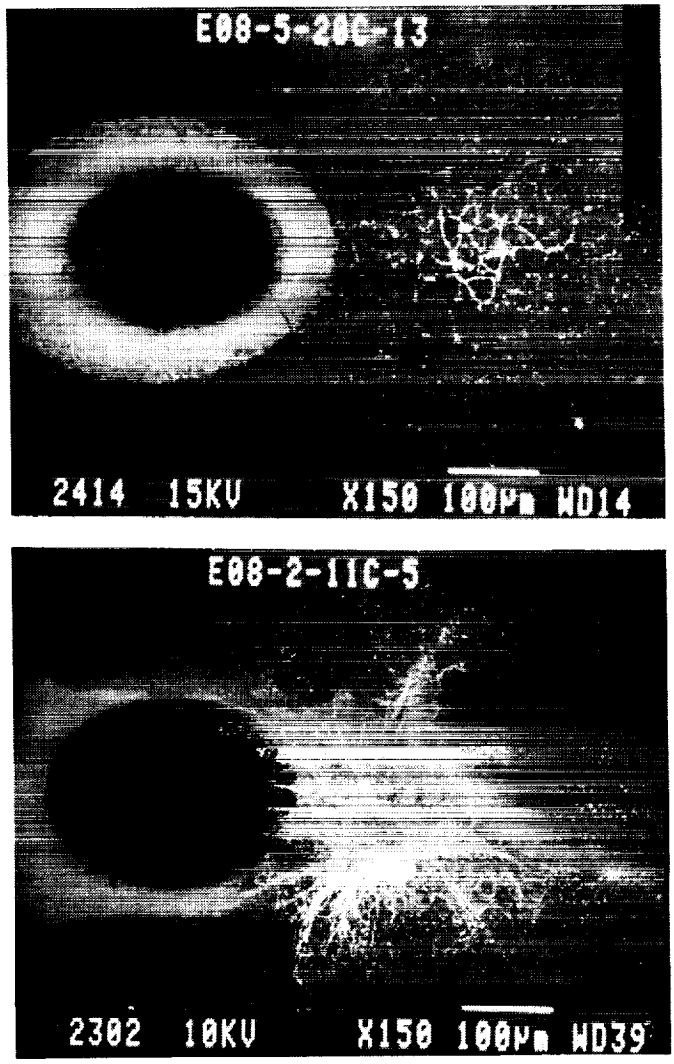

Fig. 4. Elliptical features associated with extended impacts. These multi-ringed concentric features are seen in about half of the extended impacts found in the leading edge cells. Their presence indicates that the entrance foils did not rupture immediately upon impact.

embrittlement to be a likely source of this degradation.

We plan to continue to address the question of foil lifetimes by determining the density of small craters (down to ≤1 μm diameter) that can be seen by scanning at 1000× in an SEM. A possible difficulty with this approach, however, is the observation of temporal changes of the flux of very small particles impinging on the leading edge capture cells (ref. 3).

SIMS CHEMICAL ANALYSIS OF EXTENDED IMPACTS

The procedures for the SIMS chemical analysis of projectile deposits in extended impacts have been described previously (ref.1). To summarize briefly: lateral multielement profiles across extended impacts are obtained by integrating secondary ion intensity depth profiles measured in areas 40 μm apart. From the ion signals we obtain elemental ratios by applying sensitivity factors determined from measurements on standards. Previous measurements have shown that different elements can be distributed differently in a given impact, apparently reflecting compositional heterogeneity of the projectile. While we plan to use a newly acquired secondary ion digital imaging system to determine the spatial distribution of various elements over the entire impact area, for the time being we have adopted a compromise – elemental ratio determinations from lateral profile data are estimated by taking ion intensities measured at the maximum of the $^{24}Mg^+$ signal.

During SIMS measurements of extended impacts on the Ge plates it became clear that the sensitivity of the analysis technique is not one of the limiting factors (interestingly, SEM-EDS studies of the same impacts gave no signals of projectile material, even at low voltages). The major

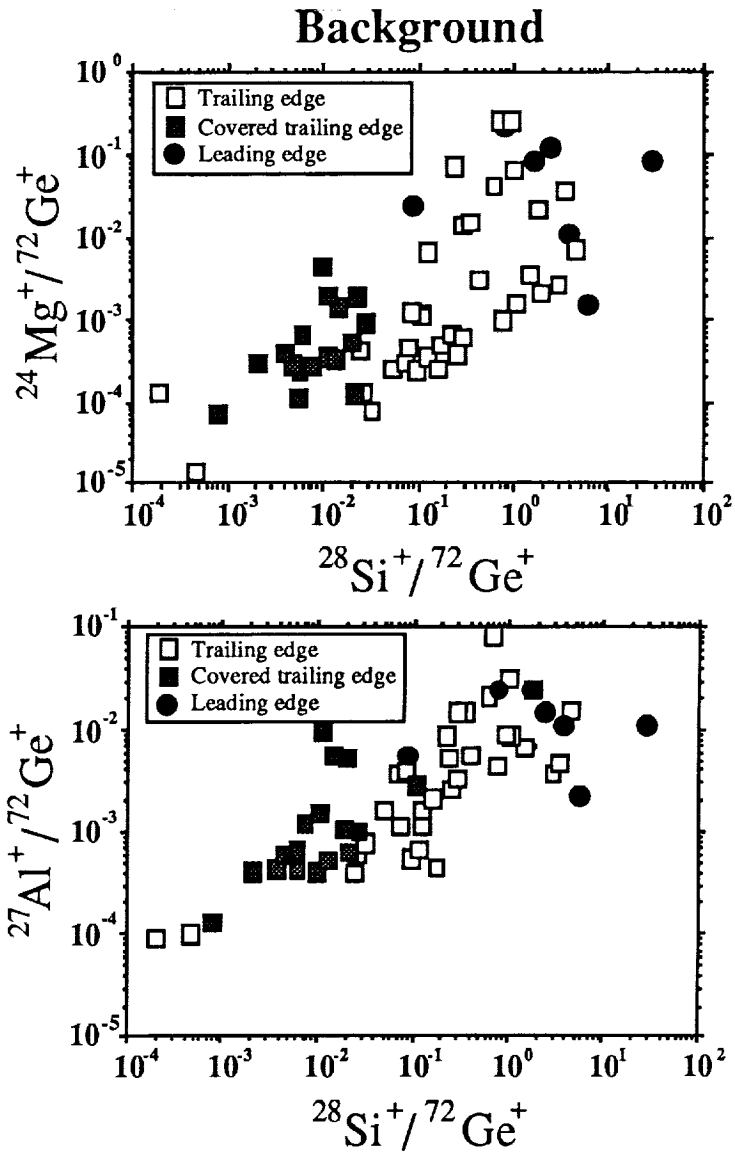

Fig. 5. Surface contamination on Ge target plates in regions well removed from impact debris.

limitation on the SIMS data is rather the high level of contamination encountered on the surface of the Ge plates. While contamination with Si is worst, high background levels are found also for other elements. Fig. 5 shows ion signals measured outside of the impact areas normalized to the $^{72}Ge^{+}$ signal. Background levels of Mg and Al are correlated with those of Si. The plots furthermore clearly show that the contamination levels are related to the exposure of the cells during flight: on average, the backgrounds are lowest on the plates from capture cells that retained their plastic foils and highest on the plates exposed on the leading edge. While we originally thought that outgassing of the RTV that was used to bond the Ge plates to the Al substrate was the main source for the Si contamination, the fact that other elements correlate with the Si demonstrates that there must be other sources of contamination. The fact that the leading edge plates have the highest background levels may be an important clue suggesting, for example, that redeposition of atomic oxygen induced erosion products may be significant.

Analysis of Impacts on the Leading Edge

To date we have performed SIMS analyses on 11 extended impacts from the leading edge. In 8 of these impacts enhancements were seen only for Al. Fig. 6 shows one of the impacts and the corresponding lateral ion intensity profiles. One additional impact showed enhancements mostly in Ti with minor Al. Its SEM micrograph and lateral ion intensity profiles are presented in Fig. 7. The remaining two impacts have hardly any elemental enhancements that can be attributed to projectile material in the region that exhibits damage features in the SEM. It has already been mentioned that the leading edge Ge plates suffer from extremely high levels of contamination (Fig. 5), and this may be the reason that no projectile material above background could be detected in these two impacts.

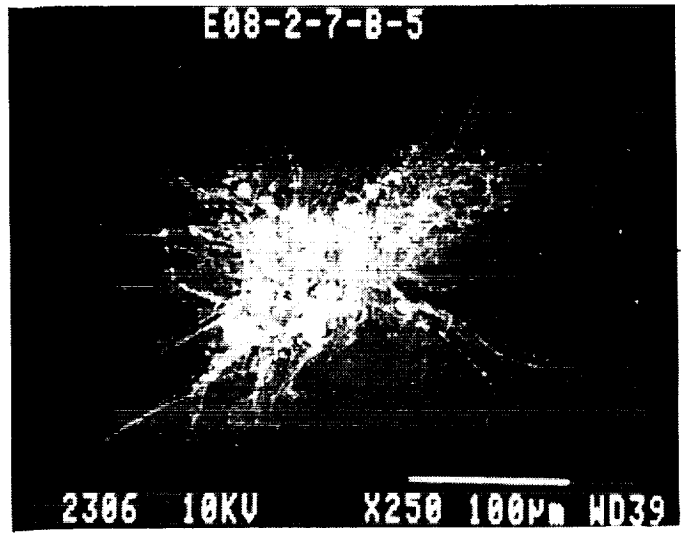

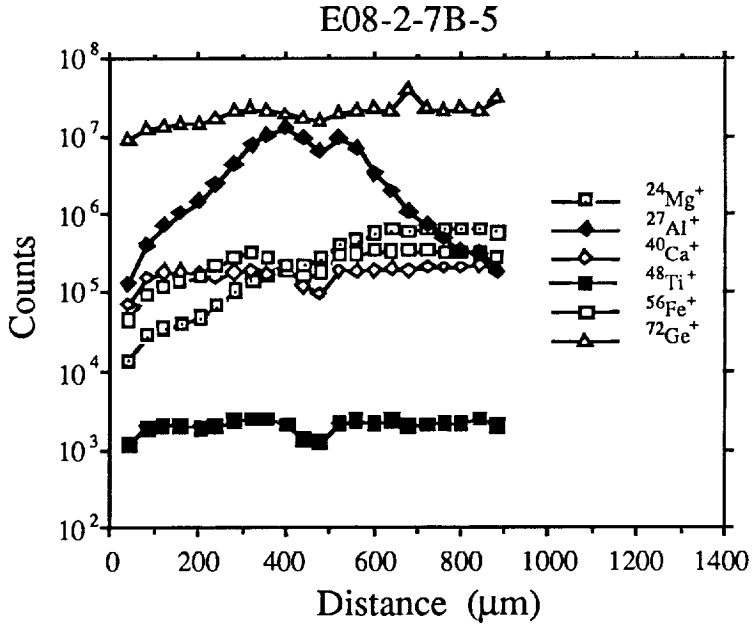

Fig. 6. Signature of an orbital debris impact found in a leading edge cell. The ion microprobe scan across impact E08-2-7B-5 shows Al as the only element that is present at enhanced levels.

The extended impacts from the leading edge capture cells thus differ significantly from those from the trailing edge capture cells in the chemical composition of their deposits. No impacts with only Al or Ti deposits such as those depicted in Figs. 6 and 7 have been seen on the trailing edge Ge plates. We can thus, with reasonable certainty, assign the 9 leading edge impacts that contain only Al or Ti to man-made debris. The first are most likely Al-oxide particles produced by solid-fuel rocket engines, the latter (mostly Ti) either is a chip of paint or a fragment of spacecraft hardware. Although the number of investigated leading edge impacts is still extremely limited, their chemical analysis shows that they are dominated by man-made debris.

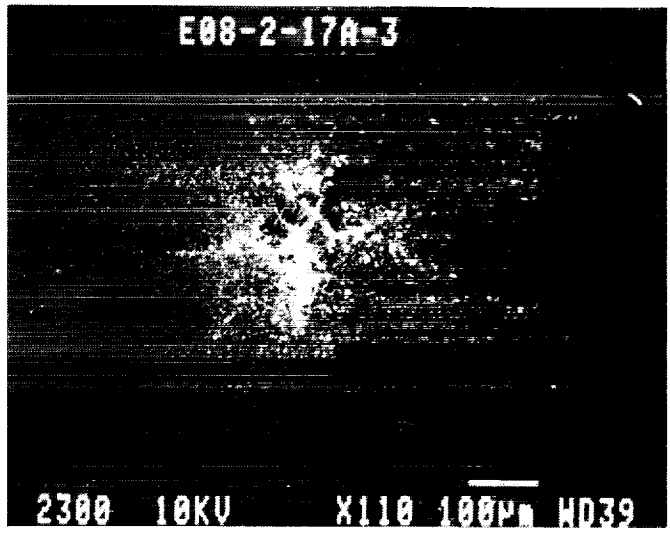

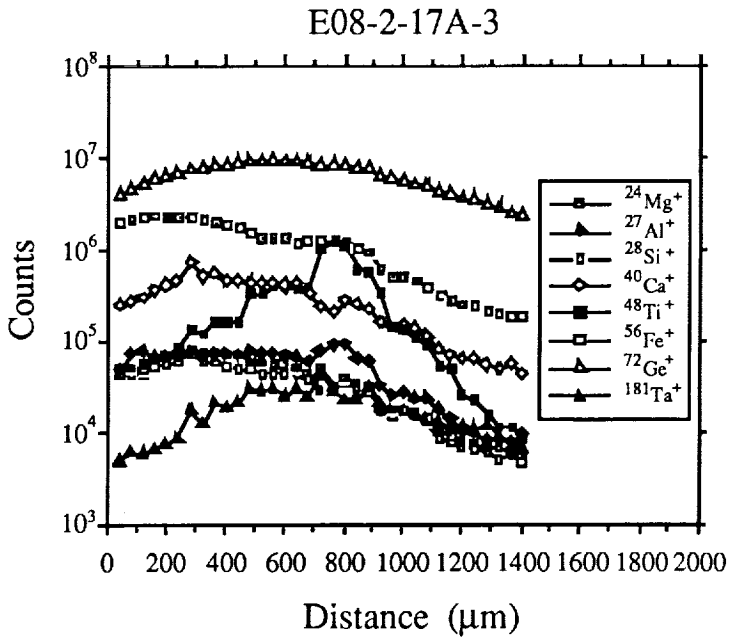

Fig. 7. Another probable orbital debris impact in a leading edge cell. The ion microprobe traverse across extended impact E08-2-17A-3 shows enhancements of both Ti and Al.

Analysis of Impacts on the Trailing Edge

In the present work, we analyzed another 16 extended impacts from the bare trailing edge capture cells (increasing the total number of impacts from these cells analyzed by SIMS to 40) and 18 extended impacts from the 12 trailing edge cells that had retained their foils. Histograms of computed elemental ratios for all impacts with clear maxima of the plotted elements in the lateral intensity profiles (32 of the bare cell impacts and 16 of the covered cell impacts) are shown in Fig. 8. They are compared with elemental ratios measured by SIMS in interplanetary dust particles collected in the stratosphere (ref. 4,5). Chondritic ratios are indicated for reference.

For the Ca/Mg, Ti/Mg and Fe/Mg ratios there appears to be no systematic difference between the impacts from the bare and covered capture cells. The Al/Mg ratios, however, are on average smaller in impacts from the covered cells than in those from the uncovered cells. A possible explanation for this discrepancy is the higher level of contamination on the exposed Ge plates (Fig. 5).

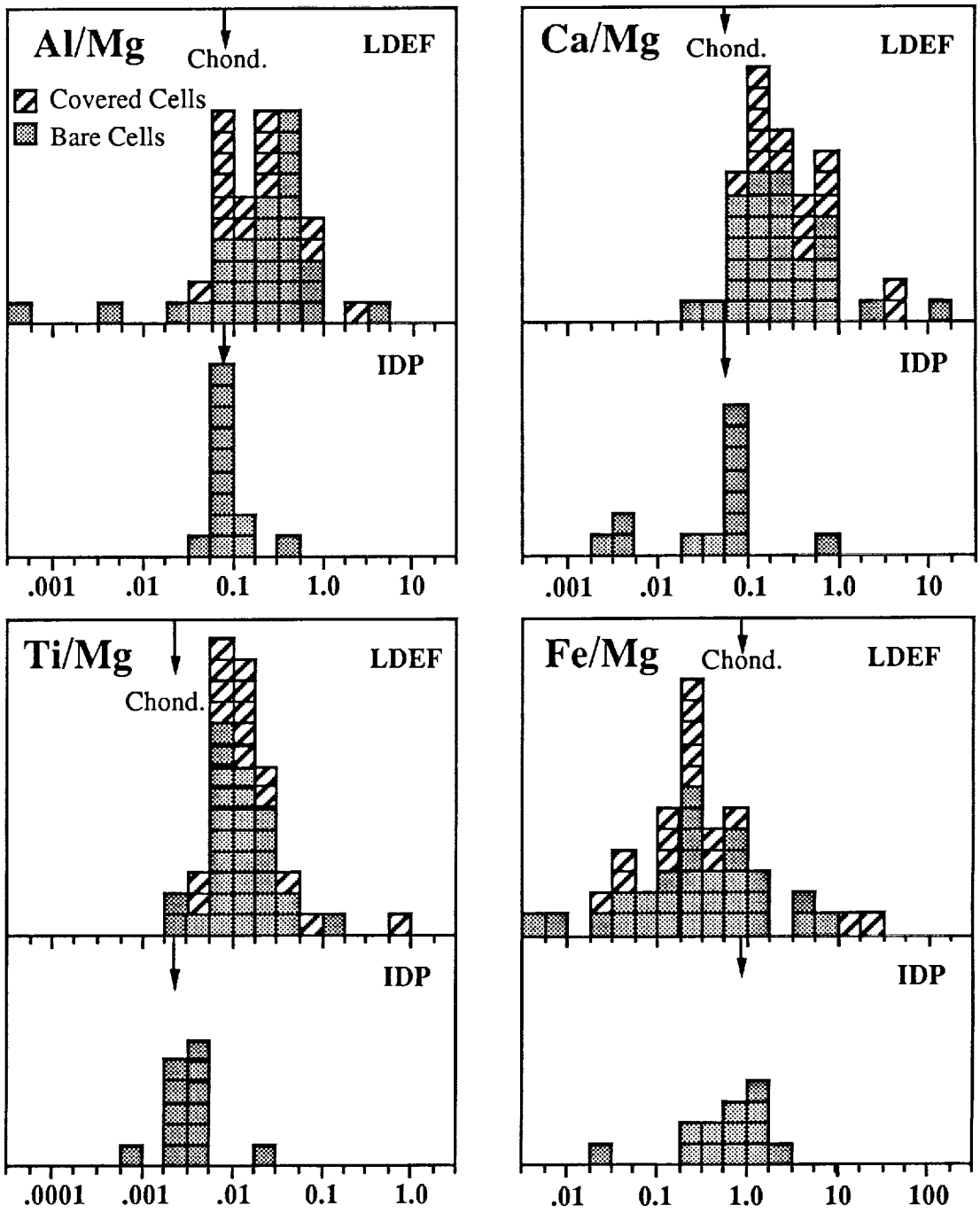

Fig. 8. Histograms of elemental ratios measured in LDEF extended impacts compared to previous measurements of a set of interplanetary dust particles (IDPs) collected in the stratosphere. Average chondritic values are indicated by the arrows.

The systematic shift of the elemental ratios measured for extended impact residues compared to IDPs and chondritic ratios has previously been noted and discussed by us (ref. 1). We pointed out that laboratory simulation experiments indicated that projectile residue material on the Ge plates is

fractionated in its elemental composition relative to the original projectile with refractory elements being enhanced in the deposits relative to less refractory elements (ref. 6). These simulation experiments on foil/Ge cells identical to those flown on LDEF also showed that the elemental fractionations are larger for material on the Ge plates than for material deposited on the backside of the entrance foil (Fig. 9).

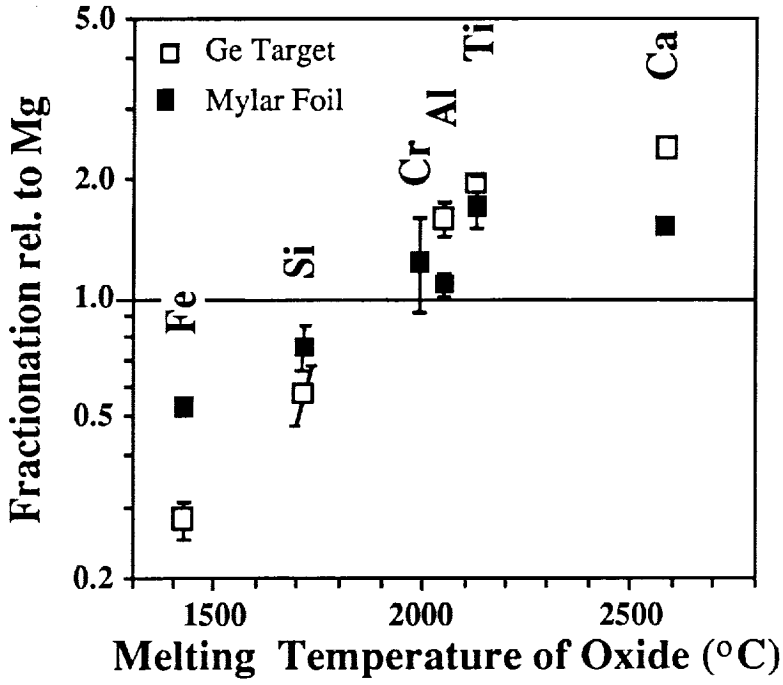

Fig. 9. Element fractionation trends measured in laboratory impact experiments. The data are from the thesis of G. Lange Heidleberg, 1986 and were obtained with the W.U. ion microprobe. The ordinate shows measurements of the relative abundance of different elements in the impact debris compared to the abundance of those same elements in the glass projectiles used in the impact experiments. The abscissa orders the elements by a volatility index.

The impacts in the covered trailing edge cell provided us with the opportunity to test this elemental fractionation effect for projectiles captured on LDEF. So far we have attempted the analysis of foil deposits from 5 impacts in the covered cells. Unfortunately, the SIMS measurements of the foils are very difficult, mostly due to extreme embrittlement of the samples and their failure to stay stretched and smooth when mounted for ion probe analysis. We obtained a good SIMS analysis on only one foil deposit of the five tried. Data for this impact are discussed next.

The extended impact on Ge and the backside of the foil featuring the penetration hole and signs of secondary ejecta are shown in Fig. 10 together with lateral profiles across the Ge impact and the deposits on the foil. The elemental ratios obtained from these profiles are plotted in Fig. 11 and compared to the fractionation of a projectile of chondritic composition expected from laboratory experiments. As expected, the material from impact EO3-2-11A-3 deposited on the Ge plate is more fractionated than the material found on the backside of the mylar foil. The relative fractionation for the LDEF impact is larger than the average obtained from the simulation experiments. This is probably a reflection of a difference in the impact velocities but could also reflect differences in chemical composition and physical properties (density, shape) of the projectile.

Although additional measurements on foil deposits are needed, the presence of elemental fractionations between Ge and foil deposits in one LDEF impact makes it likely that the dominant cause for the large differences between elemental ratios measured in extended impacts from the trailing edge and those measured in IDPs is elemental fractionation during the high velocity impact process. Intrinsic, large differences in chemical compositions between these two populations is less likely, although still possible.

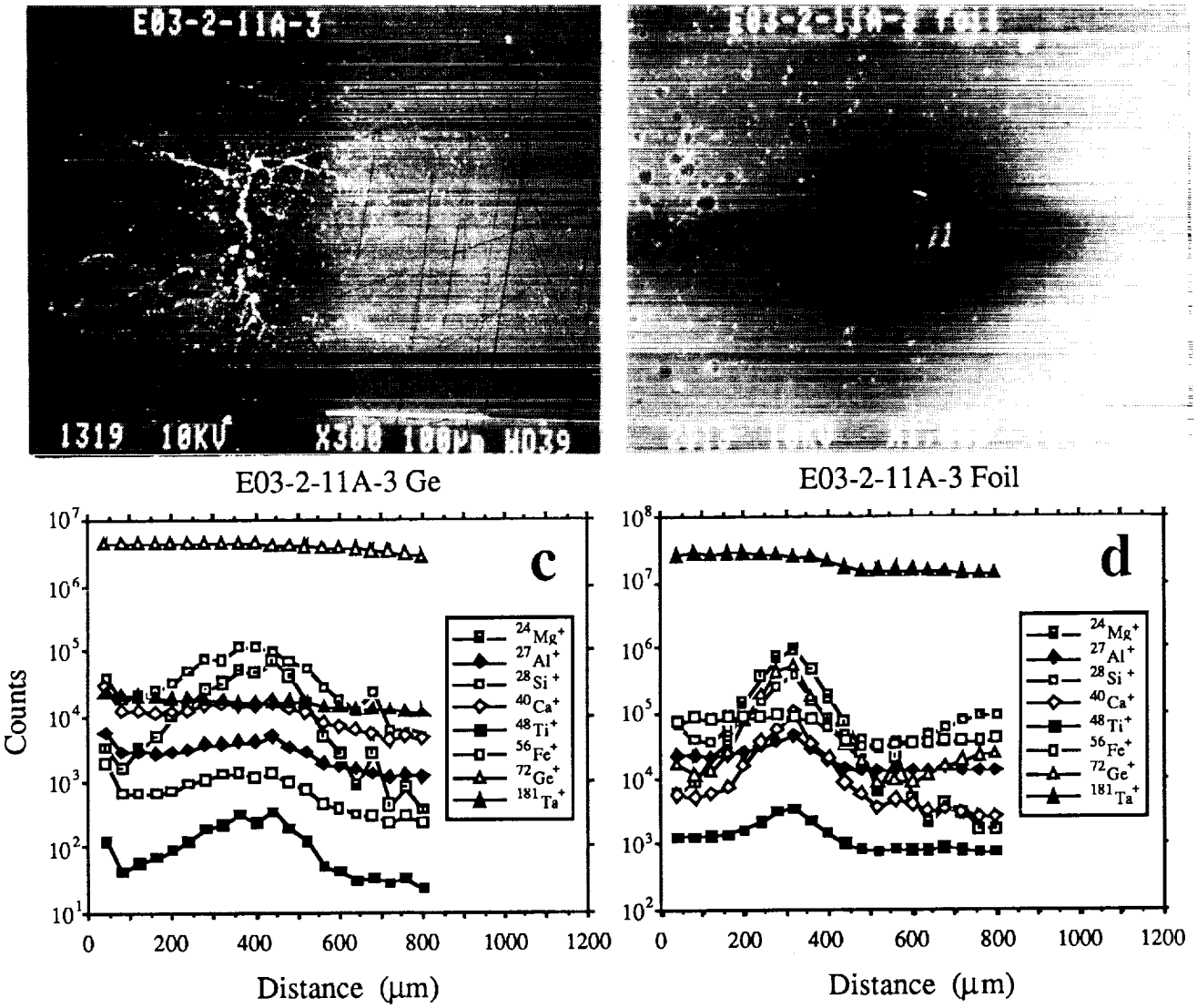

Fig. 10. Ion microprobe profiles on both the Ge target plate and the underside of the entrance foil for impact E03-2-11A-3. Most of the capture cells lost their entrance foils during flight and those that survived are extremely brittle and difficult to mount. The data shown are for the only cell for which it has been proven possible to study impacts in the way that we had originally intended. As expected from simulation experiments the projectile signals are much higher for the debris on the foil than for the debris on the Ge target plate.

The presence of elemental fractionations in the impact deposits is the single largest impediment to accurate determination of projectile chemistry. In principle, all of the projectile material, except the small fraction that escapes back through the impact hole in the entrance foil, is deposited in the capture cell, i.e. in our design either on the Ge plate or the backside of the foil. However, more volatile elements are apparently deposited over a wider area of the Ge plate and foil and, when the surface concentration becomes too low, can no longer be detected. It is therefore important to measure the surface deposits over as wide an area as possible. Measuring the radial dependence of the abundances of different elements may allow the development of normalization procedures that could correct for fractionation

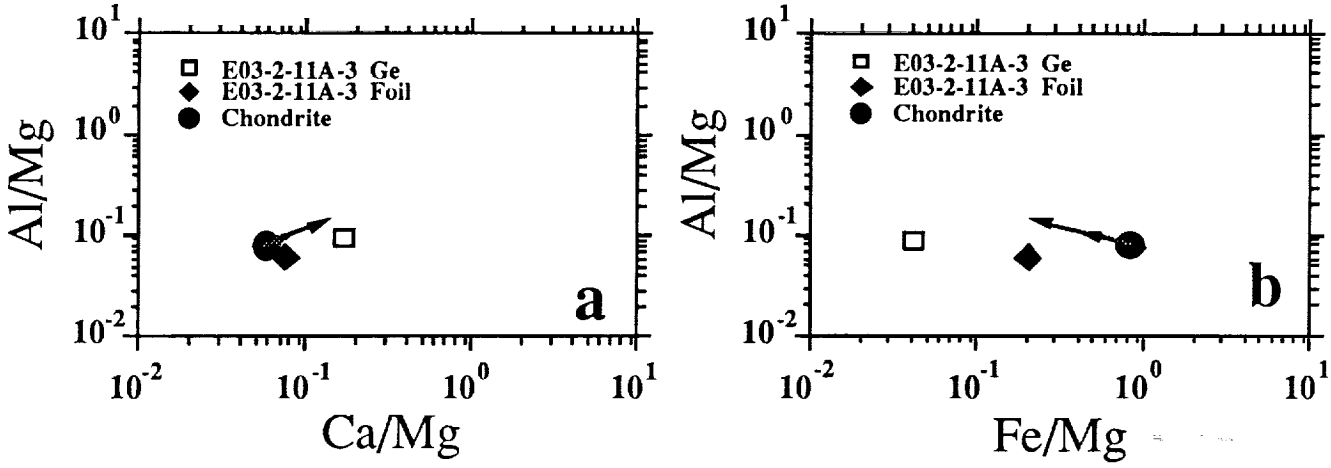

Fig. 11. Fractionation trends from the data on the intact cell shown in Fig. 10. The arrows indicate the fractionation trends previously obtained from laboratory simulation experiments of the type shown in Fig. 9. As expected from the prior work, the projectile material on the Ge plate is fractionated relative to that on the foil.

effects. In future space experiments, it would be desirable to have partitioned capture cells which would limit the area on which material from a given impact was deposited. It is not obvious, however, how to construct such a device while keeping all surfaces accessible to SIMS analysis.

IDENTIFICATION OF THE ORIGIN OF PROJECTILE MATERIAL

In spite of the problems caused by elemental fractionation the abundance data can be used to decide which LDEF impacts were caused by micrometeoroids and which ones by man-made debris. The situation is fairly simple for the extended impacts from the leading edge. Eight of these impacts show only Al enhancements and one shows Ti with minor Al and all can therefore be attributed to man-made debris with high confidence. Two impacts do not contain any clear enhancements and are thus unidentified.

The identification of the origin of trailing edge impacts is more difficult. One of them does not show any noticeable element enhancements and its origin is unidentified. Two impacts have enhancements in Fe only without any accompanying enhancements in Cr and Ni. They therefore cannot be caused by stainless steel debris particles. It is not unlikely that the projectiles are FeS particles. Such particles have been found in the stratospheric dust collection (ref. 7) and unmelted FeS fragments have been identified in LDEF craters (ref. 8). Since S is much more sensitive when measured as a negative secondary ion we do not have any S analysis yet on these two impacts but for the time being tentatively classify them as being of cosmic origin.

There are another four trailing edge impacts for which Fe is the dominant element (always discounting Si for which, as already discussed, no reliable measurements are possible because of its

extremely high contamination level). In one case the Fe is associated with Al, which makes man-made debris the most likely source for this particular impact. Although in the other three impacts Fe is very high, Mg enhancements are also clearly present. The Fe/Mg ratios are 24.8, 25.7, and 45.2, respectively. With some elemental fractionation during impact, the true Fe/Mg ratios of the projectiles are probably even higher. Although all three particles could have consisted mostly of FeS with some chondritic material attached, we cannot exclude a debris origin (Cr is low, however). The same is true for another two trailing edge impacts in which Al and Ca are dominated by contamination on the Ge plate and in which Fe/Mg is high.

The remaining 49 trailing edge impacts have their elemental ratios Al/Mg, Ca/Mg, Ti/Mg and Fe/Mg plotted in Fig. 12. Also plotted are the same ratios for interplanetary dust particles collected in the stratosphere and for chondrites. The arrows indicate the directions of elemental mass fractionation during hypervelocity

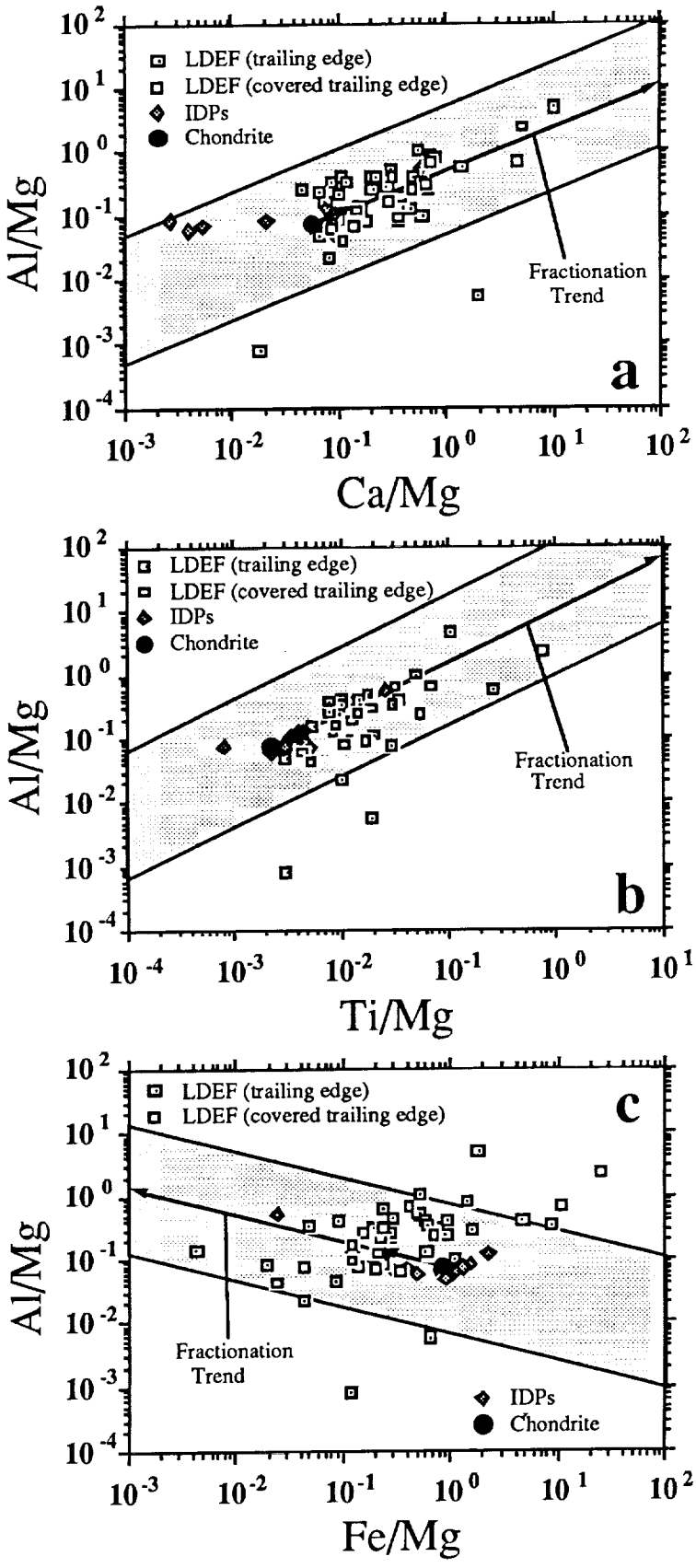

Fig. 12. Elemental ratios measured in the ion microprobe for trailing edge extended impacts. The arrows indicate elemental fractionation trends determined from laboratory simulation experiments. As discussed in the text, impacts whose compositions lie in the shaded regions are classified as "probably natural" and those outside as "possibly orbital debris." In striking contrast to the results for the leading edge cells, it appears that the majority of trailing edge impacts are produced by cosmic dust particles.

impacts determined in laboratory simulation experiments. The Al/Mg, Ca/Mg and Ti/Mg ratios of most trailing edge impacts actually deviate from the chondritic composition in the expected directions but, as already mentioned, the deviations are much larger than the fractionation seen in the laboratory experiments. We consider such large fractionations to be the likely result of the higher velocities of the LDEF impacts. As a working criterion for distinguishing between cosmic dust and man-made debris, we classify impacts that plot inside a region bounded by lines a factor of 10 above and below the fractionation trend extrapolated from laboratory experiments as being of likely interplanetary dust origin. Impacts that plot outside this region are classified as being of possibly man-made debris origin. In Figs. 12a and 12b all impacts except two plot inside of the region while in Fig. 12c, 7 plot outside.

A tentative classification of all impacts analyzed by SIMS is thus as follows (Table 2): nine of 11 leading edge impacts are of man-made origin, the origin of two impacts without projectile material cannot be identified. In contrast, 45 of 58 impacts on the trailing edge are of probably natural origin, two of them probably from FeS particles, 43 from particles with compositions similar to those of chondrites, whereas 12 impacts are possibly caused by man-made debris. It should be pointed out, however, that the identification of man-made debris is much more certain for the leading edge impacts than those from the trailing edge. The former have compositions (only Al, Ti) that are expected for debris while the debris classification for the trailing edge is mostly by default; only one impact (mostly Fe and Al) can reasonably be associated with an expected terrestrial composition and there are no impacts with Al only on the trailing edge. Thus, most of those classified as possibly man-made debris may, in fact, be cosmic particles.

Table 2. Identification of Projectile Material

	Leading edge			Trailing edge		
	Micro-meteoroids	Debris	Unid.	Micro-meteoroids	Debris	Unid.
No enhancements	-	-	2	-	-	1
Enhancement in single element	-	8 (Al)	-	2 (Fe)	-	-
Enhancement in several elements	-	1 (Ti)	-	43	12 (poss.)	-
Total	0	9	2	45	12 (poss.)	1

SUMMARY AND CONCLUSIONS

1. The basic capture cell design worked successfully. As long as the entrance foils stayed in place projectile particles produced "extended impacts" that could be successfully analyzed by ion probe mass spectrometry.

2. All of the entrance foils on the leading edge and 90% of those on the trailing edge failed during flight. However, the statistics of single craters and extended impacts show that many foils on both edges lasted for a considerable period. Thus, analysis of "extended impacts" on both the leading and trailing edges was possible.

3. Analysis of leading edge impacts shows that at least 9 of 11 impacts studied are produced by man-made debris (the remaining two did not yield any elemental enhancements due to projectile material).

4. In contrast, the analysis of the impacts on the trailing edge area shows that 45 out of 58 are of probably natural origin. The identification of the remainder is uncertain but they are possibly due to orbital debris. However, no unambiguous example of a space debris impact was found on the trailing edge.

5. Most extended impacts have compositions that differ markedly from those measured for IDPs collected in the stratosphere. The differences are consistent with volatile/refractory element fractionation affecting particles with cosmic compositions. This effect had previously been seen by us in simulation experiments of hypervelocity impacts, but is more pronounced in the LDEF data, probably due to the high velocities of the impactors. Elemental fractionation in the impact process itself represents the largest single impediment to accurate measurements of projectile chemistry.

6. Contamination of initially clean Ge surfaces during exposure in space was also found to be a significant effect limiting the ability to make accurate measurements of projectile chemistry. The source of the Si seems to be outgassing from RTV, but other sources, contributing elements such as Mg and Al, are still unknown.

7. Because leading and trailing edge entrance foils failed at comparable rates, the major causative failure factors must be similar. While atomic oxygen erosion contributed to a somewhat higher failure rate on leading edge cells, it cannot be the major cause of failure. We suspect that UV embrittlement coupled with thermal cycling is responsible for most of the foil degradation.

8. Future work will concentrate on the analysis of more leading edge impacts and the development of new techniques for measuring elemental abundances in extended impacts.

REFERENCES

1. Amari, S.; Foote, J.; Simon, C.; Swan, P.; Walker, R.; Zinner, E.; Jessberger, E. K.; Lange, G.; and Stadermann, F. J.: SIMS chemical analysis of extended impact features from the trailing edge portion of LDEF experiment AO187-2. LDEF - 69 Months in Space, NASA CP-3134, part 1; 1991, pp. 503-516.

2. Zook, H. A.: Asteroidal versus cometary meteoroid impacts on the Long Duration Exposure Facility (LDEF). Second LDEF Post-Retrieval Symposium, NASA CP-3194, 1993.

3. Mulholland, J. D.; Simon, C. G.; Cooke, W. J.; Oliver, J. P.; and Misra, V.: Long-term particle flux variability indicated by comparison of interplanetary dust experiment (IDE) timed impacts for LDEF's first year in orbit with impact data for the entire 5.75-year orbital lifetime. Second LDEF Post-Retrieval Symposium, NASA CP-3194, 1993.

4. Stadermann, F.: Rare earth and trace element abundances in individual IDPs. Lunar Planet. Sci. XXII, 1991, pp. 1311-1312.

5. Stadermann, F.: Messung von Isotopen- und Elementhäufigkeiten in einzelnen interplanetaren Staubteilchen mittels Sekundärionen-Massenspektrometrie. Ph.D. Thesis, University of Heidelberg, Germany, 1990.

6. Lange, G.: Quantitative Multielementanalyse von Einschlagsrückständen auf LDEF-Staubdetektoren. Ph.D. Thesis, University of Heidelberg, Germany, 1986.

7. Brownlee, D. E.; Tomandl, D. A.; and Olszewski, E.: Interplanetary dust; a new source of extraterrestrial material for laboratory studies. Proc. 13th Lunar Planet. Sci. Conf., 1977, pp. 149-160.

8. Brownlee, D. E.; Hörz, F.; and Bradley, J.: Interplanetary meteoroid debris in LDEF metal craters. Second LDEF Post-Retrieval Symposium, NASA CP-3194, 1993.